Journal of Computational Neuroscience 14, 239–251, 2003

Tuning Neocortical Pyramidal Neurons between Integrators and Coincidence Detectors

MICHAEL RUDOLPH AND ALAIN DESTEXHE
Unité de Neuroscience Intégratives et Computationnelles, CNRS, UPR-2191, Bat. 32-33, Avenue de la Terrasse, 91198 Gif-sur-Yvette, France
Michael.Rudolph@iaf.cnrs-gif.fr

Received April 30, 2002; Revised September 24, 2002; Accepted October 1, 2002

Action Editor: Christof Koch

Abstract. Do cortical neurons operate as integrators or as coincidence detectors? Despite the importance of this question, no definite answer has been given yet, because each of these two views can find its own experimental support. Here we investigated this question using models of morphologically-reconstructed neocortical pyramidal neurons under in vivo like conditions. In agreement with experiments we find that the cell is capable of operating in a continuum between coincidence detection and temporal integration, depending on the characteristics of the synaptic inputs. Moreover, the presence of synaptic background activity at a level comparable to intracellular measurements in vivo can modulate the operating mode of the cell, and act as a switch between temporal integration and coincidence detection. These results suggest that background activity can be viewed as an important determinant of the integrative mode of pyramidal neurons. Thus, background activity not only sharpens cortical responses but it can also be used to tune an entire network between integration and coincidence detection modes.

Keywords: cerebral cortex, synaptic background, computational model, operating mode

1. Introduction

The question of whether individual neurons encode and process information by using precise spike timings, thus, working as coincidence detectors, or spike rates, thus, working as temporal integrators, has been highly debated (e.g. Shadlen and Newsome, 1994, 1995, 1998; Softky, 1995; Softky and Koch, 1993; for conceptual issues see e.g. Koch and Laurent, 1999; Lábos, 2000; Panzeri et al., 1999, 2001a; Segundo, 2000; for a recent review see deCharms and Zador, 2000). It has been argued that the irregular firing activity of cortical neurons (experimental studies: e.g. Holt et al., 1996; Noda and Adey, 1970; Shinomoto et al., 1999; Smith and Smith, 1965; Softky and Koch, 1993; Stevens and Zador, 1998; for modeling studies see Troyer and Miller, 1997; Tsodyks and Sejnowski, 1995; Usher et al., 1994; van Vreeswijk and Sompolinsky, 1996) is inconsistent with the temporal integration of synaptic inputs, and that coincidence detection (experimental support: e.g. Gray, 1994; König et al., 1995 for cat visual cortex, Vaadia et al., 1995 for monkey frontal cortex; modeling studies: e.g. Abeles, 1982; Bernander et al., 1991; Murthy and Fetz, 1994; Softky and Koch, 1993; conceptual issues: e.g. König et al., 1996; Theunissen and Miller, 1995) is the preferred operating mode of cortical neurons. The latter emphasizes the importance of the exact timing of spikes (for experimental support: e.g. Engel et al., 1992; McClurkin et al., 1991 for visual cortex; Reinagel and Reid, 2000 for cat LGN; Bell et al., 1997; Han et al., 2000 for mormyrid electric fish; Panzeri and Schultz, 2001 for rat somatosensory cortex; Bi and Poo, 1998 for cultured neurons; Bair and Koch, 1996 for cortical area MT neurons in monkey; Prut et al., 1998 for

behaving monkey), whereas other studies (e.g. Tovée et al., 1993 for visual cortex; Barlow, 1994; Bugmann et al., 1997; Shadlen and Newsome, 1994, 1998 for modeling studies) draw attention to the temporal integration of synaptic inputs and, thus, on the importance of spike rates as the relevant coding scheme.

A series of experimental (e.g. see Krüger and Becker, 1991) and theoretical (e.g. Kretzberg et al., 2001) studies have proposed the view that cortical neurons could operate according to both of these modes, or even in a continuum between temporal integration and coincidence detection (e.g. Kisley and Gerstein, 1999; Maršálek et al., 1997 for integrate-and-fire neuron models). Here, the temporal characteristics of the input was found to be the factor determining the operating mode of the cell. When inputs are broadly distributed in time, neurons tend to respond to the average firing rate of afferent inputs. The same neurons can also respond precisely to a large number of synchronous synaptic events, therefore acting as coincidence detectors.

In between these two extremes, cortical neurons are capable of detecting an "average correlation" within a large number of random input sources (Rudolph and Destexhe, 2001a). In this type of response, the cell changes its firing rate following a change in the temporal structure of its inputs, while the afferent firing rates do not change. This response accounts for experimental situations where the only relation between single-cell discharge and behavior was the level of correlation between simultaneously recorded cells, while the firing rate of individual cells was not affected (deCharms and Merzenich, 1996; Riehle et al., 1997; Vaadia et al., 1995).

An enhancement of the ability to discriminate between synchronized or temporally dispersed stimuli was also evidenced in more detailed biophysical models with spatially extended dendritic structures and in the presence of intense synaptic noise caused by an ongoing activity in the neuronal network (Bernander et al., 1991; Maršálek et al., 1997). As for integrate-and-fire models, cells were capable of responding reliably in a broad spectrum of temporal characteristics of synaptic inputs. Interestingly, background activity allowed to tune the cellular response (Bernander et al., 1991). Moreover, it was reported that neurons effectively sharpen temporally dispersed synaptic inputs while dispersing synchronized signals, a finding which will have decisive consequences on the network level (see e.g. Diesmann et al., 1999; Shadlen and Newsome, 1998).

However, these modeling studies were performed by using either simplified models (integrate-and-fire neurons) or passive dendritic structures. This leaves the question how far conclusions about the operating mode of cortical neurons hold for the more general case of active dendrites yet unanswered. Recently, the impact of active properties on dendritic integration received a lot of attention. It was shown that in the presence of active membrane conductances qualitatively new mechanisms emerge which alter the spatiotemporal integration of synaptic inputs (for a review see Häusser et al., 2000). In this paper, we investigate the spectrum of operating modes using compartmental models of neocortical pyramidal neurons with active dendrites. Moreover, we address the question to which extend the operating mode can be controlled by other physiological signals, such as the intense synaptic background activity present in vivo.

2. Methods

Simulations were performed using a morphologically-reconstructed neocortical pyramidal layer VI neuron of a cat parietal cortex (Fig. 1A) obtained from a previous study (Contreras et al., 1997). The dendritic surface was corrected for spines under the assumption that about 45% of the dendritic membrane area are represented by spines (DeFelipe and Fariñas, 1992). Passive model parameters were adjusted to intracellular recordings obtained after application of TTX and synaptic blockers (Destexhe and Paré, 1999) and kept constant over all simulations. An intracellular resistivity of $R_a = 250\ \Omega$ cm, membrane resistivity of $R_m = 22$ k Ω cm^2 ($R_m = 50\Omega$ cm^2 in the axon), and capacitance of $C_m = 1\ \mu$F cm^{-2} ($C_m = 0.04\ \mu$F cm^{-2} in the axon) were used, where C_m was increased and R_m decreased (Holmes, 1986) by a factor of 1.45 to account for dendritic spines.

Voltage-dependent conductances were inserted in the soma, dendrites and the axon to simulate active currents (sodium current I_{Na}, delayed-rectifier potassium current I_{Kd} and voltage-dependent potassium current I_{M}). All currents were described by Hodgkin-Huxley type models (Hodgkin and Huxley, 1952) with constant peak conductance densities of $\bar{g}_{\mathrm{Na}} = 52.3$ mS cm^{-2} in dendrites ($\bar{g}_{\mathrm{Na}} = 36.1$ mS cm^{-2} in the soma, $\bar{g}_{\mathrm{Na}} = 361$ mS cm^{-2} in the axon), $\bar{g}_{\mathrm{Kd}} = 10.1$ mS cm^{-2} in dendrites ($\bar{g}_{\mathrm{Kd}} = 7$ mS cm^{-2} in the soma, $\bar{g}_{\mathrm{Kd}} = 70$ mS cm^{-2} in the axon), and $\bar{g}_{\mathrm{M}} = 0.51$ mS cm^{-2} in dendrites ($\bar{g}_{\mathrm{M}} = 0.35$ mS cm^{-2} in

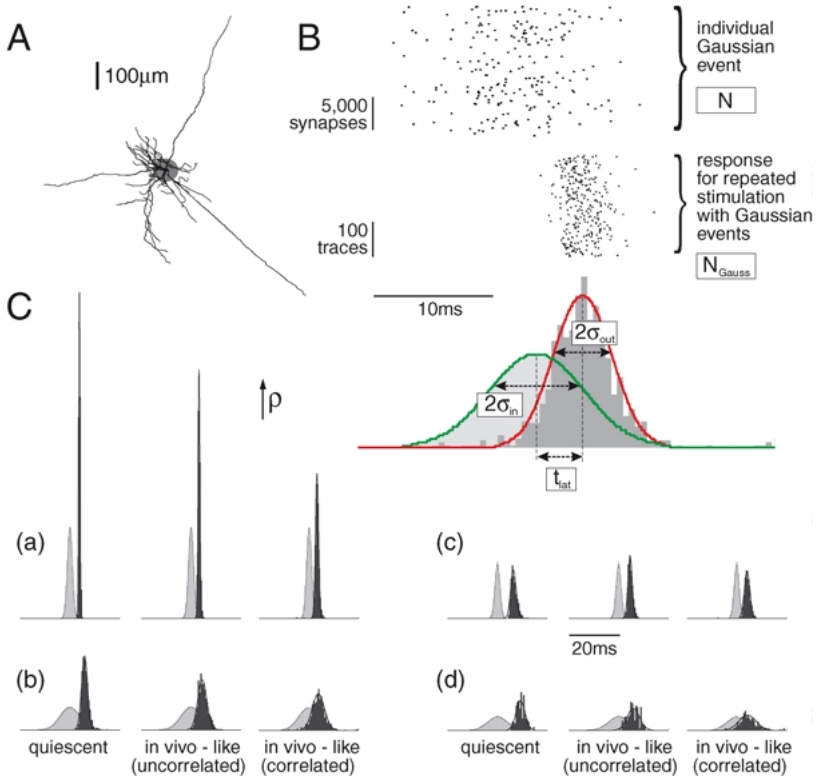

Figure 1. Simulation protocol. A: Morphologically-reconstructed neocortical pyramidal layer VI neuron of a cat used in the modeling studies. The shaded area indicates the proximal region (radius ≤ 40 μm). Inside that region there were no excitatory synapses, whereas inhibitory synapses were spread over the whole dendritic tree. B: Scheme of the simulation protocol. Individual Gaussian events (top panel) were obtained by distributing N synaptic inputs randomly in time according to a Gaussian distribution of standard deviation σ_{in} (light grey curve, bottom panel). The cellular response was recorded for repeated stimulation with N_{Gauss} individual Gaussian events (middle panel), yielding a Gaussian shaped PSTH of width σ_{out} and a mean shifted by the latency t_{lat} against the mean of the input events (dark grey curve, bottom panel). C: Representative examples of Gaussian input events (light grey) and corresponding cumulated responses (dark grey) for quiescent conditions, and under (correlated and uncorrelated) in vivo-like activity. Characteristics of Gaussian input events: (a) $N = 220$, $\sigma_{\text{in}} = 1$ ms; (b) $N = 220$, $\sigma_{\text{in}} = 4$ ms; (c) $N = 130$, $\sigma_{\text{in}} = 1$ ms; (d) $N = 130$, $\sigma_{\text{in}} = 4$ ms. The relative probability ρ is defined as $\rho =$ (number of spikes in time interval T)/($N_{\text{resp}} \times T$) (see Methods).

the soma, no I_{M} in the axon). The kinetics of the currents were taken from a model of hippocampal pyramidal cells (Traub and Miles, 1991), adjusted to match voltage-clamp data of cortical pyramidal cells (Huguenard et al., 1988). For a review about active dendrites and dendritic integration, see e.g. Johnston et al. (1996) and Magee (2000).

Synaptic currents were incorporated using two-state kinetic models of glutamate α-amino-3-hydroxy-5-methyl-4-isoxazolepropionic acid (AMPA) and γ-aminobutyric acid type-A (GABA_A) receptor types (Destexhe et al., 1998) with quantal conductances of $g_{\text{GABA}} = 869.4$ pS (distal region, $g_{\text{GABA}} = 600$ pS for proximal region, see Fig. 1A), and $g_{\text{AMPA}} = 1738.8$ pS. No metabotropic receptors were included. The densities of synapses in different regions of the layer VI cell under consideration were estimated from morphological studies in neocortical pyramidal cells (DeFelipe and Fariñas, 1992; Larkman, 1991; White, 1989), leading to a total of 16563 glutamatergic and 3376 GABAergic synapses. To perform the simulations in a time-efficient manner, an accelerating algorithm (Lytton, 1996) was used to handle synaptic conductances.

Simulations were performed by repeated synaptic stimulation with individual Gaussian events (Fig. 1B, top panel). The latter were obtained by distributing N excitatory synaptic inputs randomly across the synaptic tree, and randomly in time according to a Gaussian distribution of standard deviation σ_{in} (Fig. 1B, bottom

panel, light grey curve). The value of σ_{in} quantifies the level of simultaneity or dispersion in time of the synaptic inputs (see also Diesmann et al., 1996; Kisley and Gerstein, 1999; Maršálek et al., 1997), with a more temporally dispersed signal for larger σ_{in}, and a sharper signal (characterizing synchronous synaptic activity) for smaller σ_{in}. To examine the model neuron's spectrum of operating modes, the shape of the Gaussian input events was altered by changing the parameter values in a range $100 \leq N \leq 250$ with a stepsize $\Delta N = 10$, and $0 \text{ ms} \leq \sigma_{in} \leq 5 \text{ ms}$ with a stepsize $\Delta\sigma_{in} = 0.2$ ms.

For each parameter set, the cellular response was recorded for repeated stimulation with $N_{Gauss} = 1200$ individual Gaussian events (Fig. 1B, middle panel; simulation time of 60,000 ms for each parameter set, period of 50 ms between centers of subsequent Gaussian events, time resolution 0.1 ms). Resulting peri-stimulus time histograms (PSTHs) were normalized using the total number of stimulus evoked spikes N_{resp}, yielding the relative probability distribution

$$\rho = \frac{\text{number of spikes in time interval } T}{N_{resp} \times T},$$

and fitted with a Gaussian function (Fig. 1B, bottom panel, dark grey curve), characterized by a mean, which was shifted by the mean latency t_{lat} relative to the mean of the input events, and width σ_{out}. The latter can be viewed as a measure of the temporal dispersion of the cellular response, and compares to "precision" in Mainen and Sejnowski (1995). Examples of individual events are shown in Fig. 1C. The relation between input and output synchrony was quantified by the ratio

$$\xi = \frac{\sigma_{in}}{\sigma_{out}},$$

and the reliability of a cellular response to Gaussian events by the ratio

$$R = \frac{N_{resp}}{N_{Gauss}}.$$

Synaptic background activity was simulated by inhibitory and excitatory synapses which were driven by a Poisson process with average rates of $\nu_{inh} = 5.5$ Hz for $GABA_A$ synapses and $\nu_{exc} = 1.0$ Hz for AMPA synapses, as estimated previously based on recent data from intracellular recordings of pyramidal neurons before and after application of TTX (Destexhe and Paré, 1999; Paré et al., 1998). In some cases, a correlation among synaptic background events was introduced, resembling statistical properties evidenced in cortical networks activity in vivo (Vaadia et al., 1995; Zohary et al., 1994). To this end, independent random release events were redistributed among all synapses to increase the probability of co-release, but every terminal still released according to a Poisson process (see details in Destexhe and Paré, 1999; Rudolph and Destexhe, 2001b). The correlation used for parts of the simulations corresponds to a Pearson's correlation coefficient of about 0.1, consistent with the weak correlation found between pairs of neurons in monkey cerebral cortex (Vaadia et al., 1995; Zohary et al., 1994).

All simulations were performed using the NEURON simulation environment (Hines and Carnevale, 1997), running on DELL computers (Dell Computer Corporation, Round Rock TX, USA) under the LINUX operating system.

3. Results

We investigated the operating mode of neocortical pyramidal neurons by using morphologically-reconstructed biophysical models in which a set of input synapses was spatially distributed in dendrites. These input synapses were activated according to a Gaussian-distributed pattern whose temporal dispersion was controlled by its standard deviation σ_{in} (see Methods). This distributed synaptic stimulus was applied either in isolation (quiescent state), or in the presence of synaptic background activity. In all cases, the cellular response was quantified using PSTHs obtained by cumulating output spikes for repeated stimulations. The temporal dispersion of the output spikes generally followed a Gaussian distribution (Fig. 1C, dark grey), which was quantified by its amplitude (the total number of output spike events N_{resp}), its width (σ_{out}) and a mean latency with respect to the input distribution (t_{lat}; see Fig. 1B). The reliability R was defined as the ratio between the number of output spikes and the number of applied Gaussian events (see Methods), and the sharpening of responses was evaluated from the ratio between the standard deviations of input and output distributions ξ.

In quiescent conditions, the cell showed a reliable response ($R = 1$) to Gaussian events of nearly all widths (Fig. 2A1; see Segundo et al., 1966; Kisley and Gerstein, 1999), suggesting that the cell is capable of acting as both a coincidence detector (for small σ_{in}) or a temporal integrator (for large σ_{in}). The minimal number of synaptic inputs N required to evoke a response

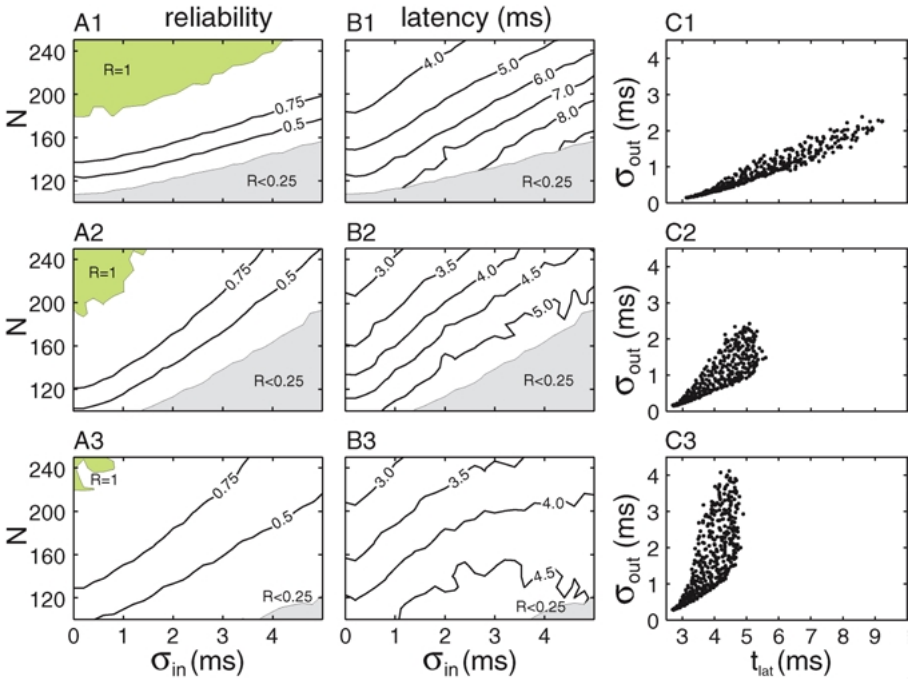

Figure 2. Cellular response as function of input parameters. A: Reliability R with which the Gaussian events drive the postsynaptic response. In the quiescent case (A1) the cell is capable of responding reliable to events of nearly all widths, whereas the region with $R = 1$ decreased in the presence of uncorrelated (A2) and correlated (A3) background activity. Moreover, under quiescent conditions, the dependence of R on the strength of the Gaussian signal N becomes weaker (smaller slope of iso-reliability lines). B: The mean latency t_{lat} as a function of Gaussian stimuli characteristics in the quiescent case (B1) and under uncorrelated (B2) and correlated (B3) in vivo-like conditions. C: Relation between t_{lat} and the output jitter. In the quiescent case (C1) there is a nearly linear relation, allowing to determine the time of the occurence of the input events by measuring the jitter of the output, whereas no corresponding relation can be evidenced under in vivo-like conditions (C2 uncorrelated, C3 correlated).

(as indicated by the boundary of the $R = 1$ region in Fig. 2A1) was lower for more synchronized input events (smaller σ_{in}). In agreement with other studies (Abeles, 1982; Aertsen et al., 1996; Bernander et al., 1991; König et al., 1996; Softky, 1995), this result indicates that coincidence detection is the more "efficient" operating mode. However, the flat boundary for $R = 1$ also shows that, in quiescent conditions, temporal integration needs only a small increase in the strength N of the temporally dispersed synaptic input in order to be effective.

This picture changed quantitatively in the presence of synaptic background activity. Here, coincidence detection was still the most efficient operating mode, but the higher slope of the boundary for $R = 1$ (see Fig. 2A2 and A3) indicates that an effective temporal integration can be obtained only for a marked increase in the strength of the temporally dispersed input signal (see also Bernander et al., 1991). For fixed N, the cell was less capable of responding reliably to Gaussian events of higher widths compared to quiescent conditions, and for correlated background activity (see Methods) a reliability of $R = 1$ was only obtained for very strong input signals (large N) with a very narrow temporal distribution ($\sigma_{\text{in}} < 1$ ms). This overall increase in the strength of the synaptic input necessary to evoke a response as well as the reduction in reliability for stronger input events (small σ_{in}, larger N; compare Fig. 2A1 and A2) must be viewed as a direct result of the smaller input resistance (or increase in the effective membrane conductance shunting the dendrites) caused by the intense synaptic background activity impinging on the cell. On the other hand, the spontaneous discharge activity shifted the parameter region with no or only low reliable responses ($R < 0.5$) towards lower input strength N. The latter effect, which can be interpreted as "enhanced responsiveness" (see e.g. Hô and Destexhe, 2000), was pronounced for correlated background activity (compare Fig. 2A2 and A3). Interestingly, both effects together yield a

weaker dependence of the reliability on the strength of the Gaussian events in the presence of background activity (as indicated by the broader "band" between $R = 1$ and $R < 0.25$ in Fig. 2A), which indicates a more "variable" response to discriminate input settings compared to the quiescent case.

The mean latency of the output with respect to the center of the input events shows that, in general, lower σ_{in} and large N lead to responses with shorter latencies (Fig. 2B). In the quiescent case (Fig. 2B1), a minimal time of about 3 to 4 ms corresponds to the average time dendritic spikes evoked by strong synaptic inputs need to propagate along the spatially extended dendritic tree and impact on the soma (Rudolph and Destexhe, 2001b). Weaker signals or signals with a broader temporal distribution need more time to be integrated, leading to a corresponding increase in t_{lat}. A clear increase of t_{lat} with σ_{in} (data not shown) suggests that somatic spikes generated by coincidence detection occur with a shorter delay than those caused by temporal integration (König et al., 1996; Shadlen and Newsome, 1995). However, the presence of background activity markedly decreased t_{lat} (between 25% for strong Gaussian events and 50% for weaker Gaussian events, compare Fig. 2B1 with Fig. 2B2 and B3), especially for higher σ_{in} values, yielding a t_{lat} which was much less dependent on σ_{in} and N and, thus, the operating mode for correlated background activity. This behavior could have a significant impact on the temporal resolution of subsequent Gaussian events.

In the quiescent state, tightly synchronized input distributions (small σ_{in}) caused less jitter in the timing of output spikes (Fig. 3A1) with a σ_{out} considerably smaller than σ_{in} (Fig. 3C1), in agreement with previous models (Kisley and Gerstein, 1999; Maršálek et al., 1997). However, σ_{out} depends much more on N than in passive models. It is interesting to note that σ_{out} is highly correlated and nearly proportional to t_{lat} in

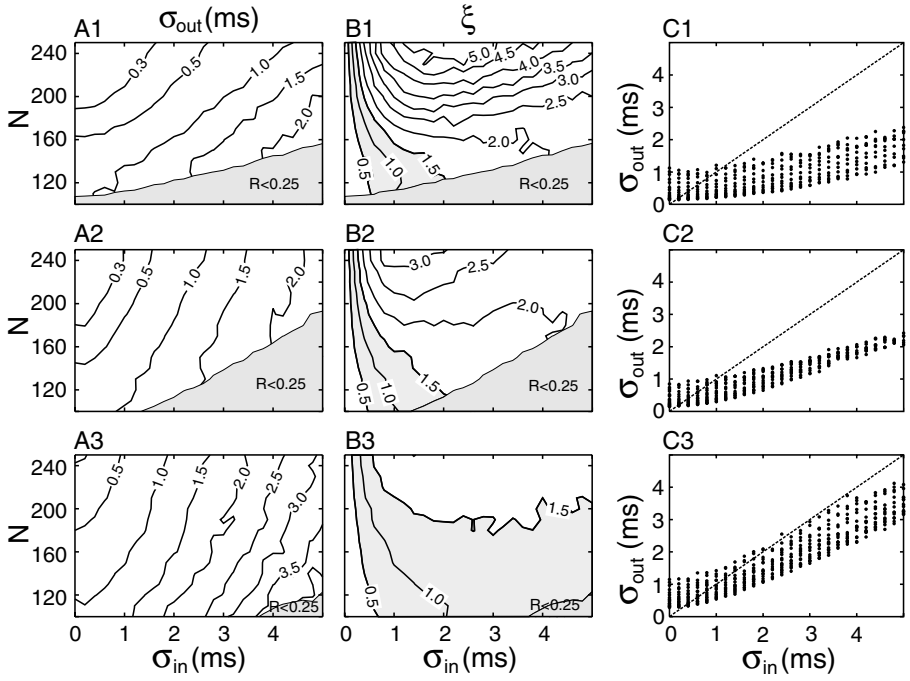

Figure 3. Synchronization of cellular response as function of synaptic input characteristics. A: Output jitter σ_{out} as a function of the input settings. In all three cases σ_{out} is lower than σ_{in} for most of the parameter range. Moreover, the dependence of σ_{out} on N is higher in the quiescent case (A1), whereas the output jitter becomes nearly independent on N in the presence of correlated background activity (A3; indicated by higher slope of iso-σ_{out} lines). A2 shows the corresponding results for uncorrelated background activity. B: $\xi = \sigma_{in}/\sigma_{out}$ as a function of the input settings. In all three cases, the input parameter range covers settings for which $\xi \sim 1$ (increasing light grey region). This range markedly increases for the correlated case (B3). B1 and B2 show the results for quiescent and uncorrelated in vivo-like conditions, respectively. C: Relation between output jitter and the synchrony in the input. In all three cases (C1 quiescent, C2 in vivo-like uncorrelated, C3 in vivo-like correlated) σ_{out} is nearly proportional to σ_{in}, but with a slope smaller than one. Only in the correlated case the slope is close to unity, suggesting a neuronal response which preserves the synchrony in the input signal.

quiescent conditions (Fig. 2C1). This behavior changed qualitatively in the presence of synaptic background activity. In addition to the overall decrease of t_{lat}, the range of σ_{out} increased with the background correlation. There was no longer a linear relation between t_{lat} and σ_{out} (Fig. 2C2 and C3). The output jitter σ_{out} depended more on σ_{in}, whereas the dependence on N became weaker (higher slope of the σ_{out} contours in Fig. 3A2 and A3, compare to Fig. 3A1).

Interestingly, although an increase in the input jitter for fixed N naturally results in stronger dispersion of the output distribution (see Fig. 3A), a weak relation between σ_{out} and the strength of the Gaussian input event could be evidenced. Here, for fixed σ_{in}, an increase in N led to a decrease in σ_{out} for both quiescent and active conditions (Fig. 3A, see also Fig. 1C). This dependency can be explained by the fact that stronger synaptic inputs lead to a depolarization with larger amplitude which drives the membrane faster to firing threshold. This, in turn, results in an effective decrease of the average latency for increasing N and fixed input dispersion σ_{in} (see Fig. 2B) as well as a sharpening of the response distribution, i.e. a decrease in σ_{out}.

To directly analyze the impact of the input synchronization on the output jitter of the cell, we investigated the behavior of the ratio $\xi = \sigma_{in}/\sigma_{out}$. The input parameter range for which $\xi \geq 1$ was large under quiescent conditions (Fig. 3B1), and only minimally changed in the presence of background activity (Fig. 3B2 and B3). However, background activity and correlation markedly lowered ξ, as indicated by the increasing light grey region in Fig. 3B2 and B3). In all cases σ_{out} was roughly proportional to σ_{in} with a slope smaller than one in the quiescent state or in the presence of uncorrelated background activity (Fig. 3C1 and C2). Only with correlated background activity the slope increased and was close to one for a broad range of input settings (Fig. 3C3), suggesting that under these conditions the cell nearly *conserves the synchronization of the input signal*. The output jitter for fixed σ_{in} stayed nearly constant in all cases for all N, with σ_{out} showing a much higher variability when synaptic background activity was present (data not shown). Interestingly, there was a relation between output jitter and reliability of the response in the presence of background activity (Fig. 4A2 and A3): a higher jitter in the output, hence less precision, is accompanied by a decrease in reliability. No such relation could be evidenced in the quiescent state (Fig. 4A1).

In order to resolve the ambiguity resulting from the fact that an output spike can be generated by an arbitrary number of synaptic inputs distributed narrowly or by integrating more synaptic events distributed diffusely in time, we investigated the slope of the membrane potential V_m preceding a spike (Kisley and Gerstein, 1999). However, only for strong inputs (high N, small σ_{in}) the slope depended on the characteristics of the input signal (Fig. 4B), with a higher sensitivity to the degree of synchrony than to N. For higher σ_{in} as well as for additional background activity, this sensitivity decreased rapidly, and the V_m slope stayed nearly constant at around 6 mV/ms (Fig. 4C). We conclude that, in contrast to passive models (e.g., Kisley and Gerstein, 1999), here the V_m slope can be used to discriminate Gaussian input settings only in a narrow range. This result is not surprising, because the Gaussian input events do not cause a somatic response directly, but rather are integrated by a spatially extended active dendritic tree before impacting the soma. Thus, the spiking response of the cell is mainly governed by the intracellular kinetics, leading to a V_m slope preceding a spike which is nearly independent of the input. A weak "inverse" correlation between the temporal precision of the output and the V_m slope was only observed in the quiescent state (data not shown).

Finally, we investigated the variability of the spiking response of the cell, quantified by the coefficient of variation C_V, defined as the ratio between the standard deviation of interspike interval and the mean interspike interval. As expected, during quiescent conditions, the periodically applied Gaussian events lead to a low C_V (Fig. 5A1), indicating a rather regular response. The increase of the C_V for low N and higher σ_{in} can be related to the lower reliability and, thus, failures of response due to weak inputs in this parameter range. This situation changed when the cell was subject to uncorrelated background activity (Fig. 5A2). Here we observed an increase in the variability for higher σ_{in} and N. However, this increase of the C_V is directly related to the change in the reliability (see Figs. 2A2 and 5A2). In contrast, in the presence of correlated background activity, the C_V was larger than zero even for $R = 1$ (Fig. 5A3 and B). This way, even for a strong periodic input stimulus, the addition of a weak background activity makes the timing of output spikes more variable, while preserving the synchronization of the input signal (see above). This result suggests that the fluctuating intracellular activity due to synaptic background activity present in the in vivo state facilitates a neuronal

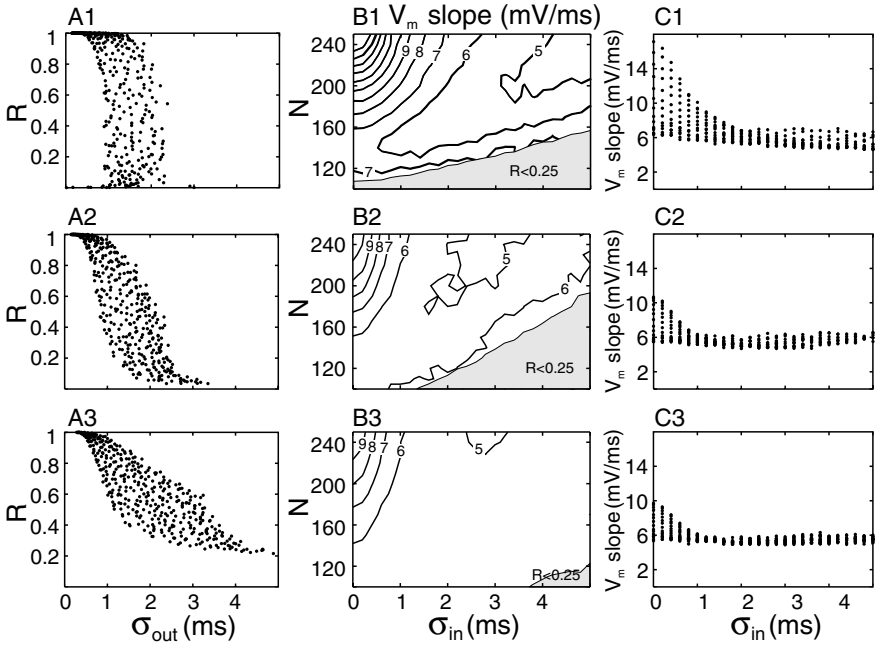

Figure 4. Impact of input parameters on the spike shape. A: Reliability R as a function of the output jitter σ_{out} for the quiescent case (A1), and in the presence of uncorrelated (A2) and correlated (A3) synaptic background activity. Under quiescent conditions there is no clear relation between both quantities, whereas correlated background activity leads to a response behavior with decreasing reliability for increasing output jitter. B: V_m slope 2 ms preceding the spike as a function of the input parameters. Only in the quiescent case (B1) for small σ_{in} and high N a weak relation can be observed, which allows to deduce characteristics of the input signal by a measurement of the V_m slope. Under in vivo-like conditions (B2 uncorrelated case, B3 correlated case) there is no longer a clear dependence. C: V_m slope 2 ms preceding spike as a function of σ_{in}. In all three cases, for weak input signals (higher σ_{in}) the V_m slope is constant (C1 quiescent, C2 in vivo-like uncorrelated, C3 in vivo-like correlated).

response which preserves the temporal precision of the input signal, while at the same time exhibiting a high interspike interval variability (see also Nowak et al., 1997a).

4. Discussion

In this paper we have investigated the operating modes of cortical neurons by using multisynaptic inputs whose dispersion in time was varied. We report three findings: First, the neuron is able to operate as an integrator or a coincidence detector depending on the characteristics of the input signal, namely the degree of synchrony in the multisynaptic input pattern. Second, there was no discrete boundary between these two operating modes, suggesting that the cell rather operates in a continuum between temporal integration and coincidence detection. Both findings are in agreement with previous studies (e.g. Aertsen et al., 1996; Diesmann et al., 1999 for feedforward networks, Kisley and Gerstein, 1999 for leaky integrate-and-fire neurons), but extend to the more biophysical situation of spatially extended dendritic structures and conductance-based intracellular activity. Third, the presence of synaptic background activity, at a level comparable to measurements in cat parietal cortex in vivo (Destexhe and Paré, 1999; Paré et al., 1998), had a decisive impact on the operating mode of the modeled cell. It led to a better discrimination of the temporal characteristics of synaptic inputs (Fig. 2A) and an overall faster response (Fig. 2B) compared to the quiescent state. Changes in statistical properties of the synaptic background also allowed to modulate the temporal characteristics of the output by changes in the temporal dispersion of the response for a given input synchrony (Fig. 3). Thus, in order to understand the operating mode of cortical cells under in vivo conditions, both the signal and (spontaneous) background activity must be taken into account as two components of the overall synaptic input pattern received by the cell.

In a previous study (Bernander et al., 1991), the effect of synaptic background activity on the spatiotemporal integration of synaptic inputs in single layer V

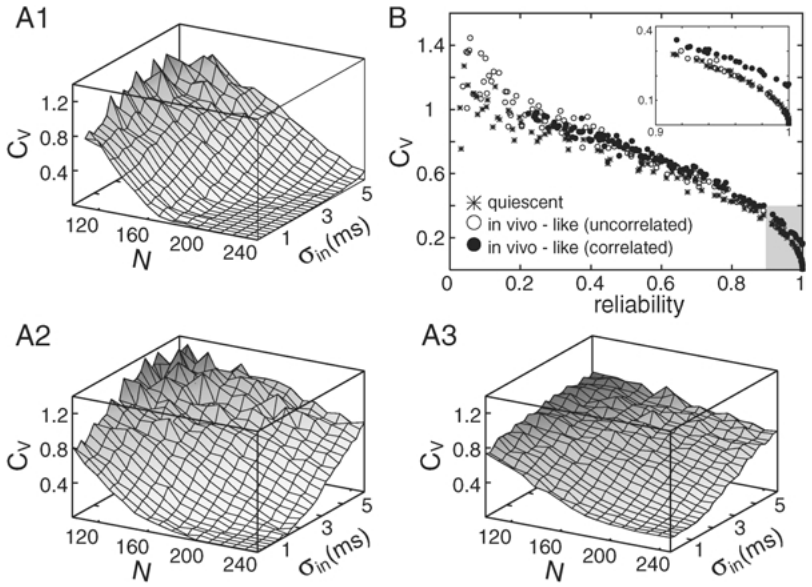

Figure 5. Variability of cellular response. A: The variability of the spiking response C_V as a function of input settings. Under quiescent conditions (A1), only weak events yield a high C_V, corresponding to the fact that weak signals mainly fail to evoke responses. For uncorrelated background activity (A2) the C_V increased for high σ_{in} due to the fact that weak input signals now interfere with a weak spontaneous firing activity. Interestingly, for the correlated background activity (A3), even very strong periodic Gaussian input signals yield a higher C_V. B: Relation between reliability R and the coefficient of variation for all three investigated cases. High reliable responses lead to less variability to the periodic input events. For correlated background activity, even for $R = 1$ the C_V is unequal zero due to the spontaneous firing activity. The grey region marks the variable range shown by the inset.

pyramidal cells with passive dendrites was investigated. Synaptic background was modeled by thousands of spatially distributed excitatory and inhibitory synaptic inputs activated randomly according to independent Poisson processes. In contrast to our study, the firing rate was changed in order to modulate the strength of the background activity. In accordance with our findings, significant changes in the cellular response to temporally synchronized or dispersed synaptic inputs were found. First, the minimal number of excitatory synapses necessary to trigger a response of the cell increased in the presence of background activity, especially for temporally dispersed inputs. This compares to Fig. 2A1 and A2, where for fixed σ_{in} a reliable response ($R \sim 1$) was only obtained for stronger inputs (larger N), a direct result of the overall smaller input resistance under in vivo conditions. Second, for fixed synaptic background activity and input strength, more synchronized synaptic inputs trigger a cellular response with higher reliability (see Fig. 2A1 to A3, decrease in R for increasing σ_{in} and fixed N). This indicates that cortical cells in vivo act preferably as coincidence detectors, but that the response to synaptic inputs with specific temporal dispersion can also be tuned by network activity.

Synaptic background activity shapes the spatiotemporal integration of synaptic inputs through changes in the electrophysiological characteristics of the cell. These changes include a decrease in the membrane time constant, an enhanced attenuation of EPSPs and a depolarized membrane potential bringing the cell closer to firing threshold. Our study differs from previous ones (e.g. Bernander et al., 1991) by showing a modulating effect of synaptic background activity on the timing of the response by a variation of the statistical properties of the synaptic background activity for fixed background frequency and, thus, membrane time constant. This approach is supported by recent experimental findings which have shown that in the awake state the cortical network can display rapid changes in the correlation between the discharge activity of individual neurons without modulation of their average firing rate (deCharms and Merzenich, 1996; Riehle et al., 1997; Vaadia et al., 1995). A detailed investigation of the interplay between changes in correlation and cellular response modulation (Riehle et al., 1997) constitutes an interesting direction for future studies.

Recently it was pointed out (see deCharms and Zador, 2000 and references therein) that the principled

question of whether neurons encode information as integrators (rate-coding) or as coincidence detectors (temporal-coding) is merely one of time scales in the addressed problem rather than one of category. Here, in agreement with studies of passive models (Kisley and Gerstein, 1999; Maršálek et al., 1997), we suggest another view, namely that the operating mode and, thus, the coding scheme, is merely one of "information contents". Both a temporally sharp signal, caused by synchronous or correlated synaptic activity, as well as synaptic signals dispersed in time, caused by a change in the presynaptic firing rate, can lead to reliable responses in a continuum between integration, utilizing more imprecise spike responses, and coincidence detection, utilizing rather precise spike times.

Synaptic background activity was found to modulate and control the integrative mode of individual cells by allowing to tune the (temporal) characteristics of their outputs. As we have shown here, changes in the correlation of the presynaptic activity alter the reliability of the response as well as the ability of the cell to discriminate between synaptic inputs arriving simultaneously or dispersed in time (Fig. 2A). Furthermore, the impact of background activity on the latency of the response suggests that the time needed for integrating synaptic inputs and, thus, the "speed" of propagation of information across cortical layers is not fixed but can be tuned by changes in the background activity (Fig. 2B). The temporal dispersion of the response was found to depend on the characteristics of background activity (Fig. 3A), which could provide a mechanism through which the cell can focus on specific temporal patterns in its synaptic inputs. Taken together, these results suggests that information contents is not only a property of the signal itself, but also depends on background activity, which is widely viewed as noise. Both signal and background activity should therefore be considered together when investigating information processing paradigms of neocortical neurons.

In this context, an enhancement in the bandwidth of information processing capability appears as a natural consequence. By modulating their firing rate, individual neurons can resolve in a specific way slow changes in the synchronous synaptic activity which are viewed to play a role in binding together the activity in different cortical regions. By responding to fast and brief changes in the synchrony of the presynaptic activity, single neurons are able to resolve signals which are viewed to play a role in coding the spatiotemporal structure of sensory stimuli. In agreement with other experimental and theoretical studies (Abeles, 1982; Aertsen et al., 1996; Bernander et al., 1991; König et al., 1996; Softky, 1995), we found that coincidence detection appears to be the more "efficient" operating mode due to the lower number of synaptic inputs required to evoke a response.

A weak correlation between the degree of synchrony in the input and the slope of the V_m preceding a spike was obtained only without background activity. The argumentation that more synchronous events will open more synaptic conductances simultaneously which drive the V_m more rapidly to threshold (Nowak et al., 1997b) does not hold in the case of spatially distributed synaptic input patterns. In addition, the active voltage-dependent conductances impact on the dendritic integration of the input signal (see for instance Schwindt and Crill, 1997; Softky, 1994, 1995; Stuart et al., 1997), leading only to a weak dependence of the V_m slope on the input characteristics. An inverse proportionality of the V_m slope to the variance of the ISI, as shown analytically (Stein, 1967), could not be confirmed in the case investigated here.

Finally, the finding of $\sigma_{\text{out}} < \sigma_{\text{in}}$ (e.g. Maršálek et al., 1997) may have important consequences at the network level. A first possible interpretation (Maršálek et al., 1997) is that the relation between input and output jitters will determine the synchronization of discharges across successive layers of interconnected neurons. If $\sigma_{\text{out}} < \sigma_{\text{in}}$, the signal becomes temporally more precise as it proceeds through the layers, but the information about the input jitter gets lost (see Abeles et al., 1993; Diesmann et al., 1999; Gerstein et al., 1989; MacGregor, 1991). This is also accompanied by a change of operating modes at different levels of the network. Here, we have shown that the ratio between σ_{out} and σ_{in} also depends on the strength and statistics of the background activity. It is close to one in the presence of correlated background activity, suggesting that in such states the synchrony of the input signal is conserved across successive layers of the cortical network. This model therefore predicts that networks can tune their operating mode by modulating the level of spontaneous activity, and that the processing of precisely timed afferent information will be possible only under specific states of network activity.

We suggest here another possible interpretation, namely to relate the input and output jitters not to successive layers, but to successive cycles of an oscillation within the same network. The latencies between input and output distributions are of the order of 3 to 8 ms

(Fig. 2C), which would correspond to fast oscillations of 120–300 Hz, such as that found in the hippocampus (Buzsaki et al., 1992), or slower oscillations if synaptic delays are taken into account. According to this scheme, the successive cycles of the oscillation would perform successive "iterations" through recurrent excitatory connections. The discharges can become more and more synchronized from cycle to cycle ($\sigma_{out} < \sigma_{in}$), conserve synchrony ($\sigma_{out} = \sigma_{in}$), or progressively loose their initial synchrony ($\sigma_{out} > \sigma_{in}$). The present results suggest that background activity (which could be generated either externally or by a subset of neurons not participating to the oscillation) would completely determine the time evolution of the synchrony and therefore the result of this "iteration". Future network models are needed to investigate further this type of dynamics, and possible relations with the physiology and roles of cortical oscillations (see Gray, 1994).

Acknowledgments

Research supported by CNRS and the National Institutes of Health (R01-NS37711).

References

Abeles M (1982) Role of the cortical neuron: Integrator or coincidence detector? Isr. J. Med. Sci. 18: 83–92.

Abeles M, Bergman H, Margalit E, Vaadia E (1993) Spatiotemporal firing patterns in the frontal cortex of behaving monkeys. J. Neurophysiol. 70: 1629–1638.

Aertsen A, Diesmann M, Gewaltig MO (1996) Propagation of synchronous spiking activity in feedforward neural networks. J. Physiology (Paris) 90: 243–247.

Bair W, Koch C (1996) Temporal precision of spike trains in extrastriate cortex of the behaving macaque monkey. Neural Computation 15: 1185–1202.

Barlow H (1995) The neuron doctrine in perception. In: MS Gazzaniga, ed. The Cognitive Neurosciences. MIT Press. pp. 415–435.

Bell CC, Han VZ, Sugawara Y, Grant K (1997) Synaptic plasticity in a cerebellum-like structure depends on temporal order. Nature 387: 278–281.

Bernander Ö, Douglas RJ, Martin KAC, Koch C (1991) Synaptic background activity influences spatiotemporal integration in single pyramidal cells. Proc. Natl. Acad. Sci. USA 88: 11569–11573.

Bi GQ, Poo MM (1998) Synaptic modifications in cultured hippocampal neurons: Dependence on spike timing, synaptic strength, and postsynaptic cell type. J. Neurosci. 18: 10464–10472.

Bugmann G, Christodoulou C, Taylor JG (1997) Role of temporal integration and fluctuation detection in the highly irregular firing of a leaky integrator neuron model with partial reset. Neural. Comp. 9: 985–1000.

Buzsaki G, Horvath Z, Urioste R, Hetke J, Wise K (1992) High-frequency network oscillation in the hippocampus. Science 256: 1025–1027.

Contreras D, Destexhe A, Steriade M (1997) Intracellular and computational characterization of the intracortical inhibitory control of synchronized thalamic inputs in vivo. J. Neurophysiol. 78: 335–350.

deCharms RC, Merzenich MM (1996) Primary cortical representation of sounds by the coordination of action-potential timing. Nature 381: 610–613.

deCharms RC, Zador A (2000) Neural representation and the cortical code. Annu. Rev. Neurosci. 23: 613–647.

DeFelipe J, Fariñas I (1992) The pyramidal neuron of the cerebral cortex: Morphological and chemical characteristics of the synaptic inputs. Prog. Neurobiol. 39: 563–607.

Destexhe A, Mainen ZF, Sejnowski TJ (1998) Kinetic models of synaptic transmission. In: C Koch, I Segev, eds. Methods in Neuronal Modeling, 2nd edn. MIT Press, Cambridge, MA. pp. 1–26.

Destexhe A, Paré D (1999) Impact of network activity on the integrative properties of neocortical pyramidal neurons in vivo. J. Neurophysiol. 81: 1531–1547.

Diesmann M, Gewaltig MO, Aertsen A (1996) Characterization of synfire activity by propagating "pulse packets." In: JM Bower, ed. Computational Neuroscience. Academic Press, San Diego. pp. 59–64.

Diesmann M, Gewaltig MO, Aertsen A (1999) Stable propagation of synchronous spiking in cortical neural networks. Nature 402: 529–533.

Engel AK, König P, Kreiter AK, Schillen TB, Singer W (1992) Temporal coding in the visual cortex: New vistas on integration in the nervous system. Trends Neurosci. 15: 218–226.

Gerstein GL, Bedenbaugh P, Aertsen AMHJ (1989) Neuronal assemblies. IEEE Trans. Biomed. Eng. 36: 4–14.

Gray CM (1994) Synchronous oscillations in neuronal systems: Mechanisms and functions. J. Comput. Neurosci. 1: 11–38.

Han VZ, Grant K, Bell CC (2000) Reversible associative depression and nonassociative potentiation at a parallel fiber synapse. Neuron 27: 611–622.

Häusser M, Spruston N, Stuart GJ (2000) Diversity and dynamics of dendritic signaling. Science 290: 739–744.

Hines ML, Carnevale NT (1997) The NEURON simulation environment. Neural Computation 9: 1179–1209.

Hô N, Destexhe A (2000) Synaptic background activity enhances the responsiveness of neocortical pyramidal neurons. J. Neurophysiol. 84: 1488–1496.

Hodgkin AL, Huxley AF (1952) A quantitative description of membrane current and its application to conduction and excitation in nerve. J. Physiol. 117: 500–544.

Holmes WR (1986) Cable theory modeling of the effectiveness of synaptic inputs in cortical pyramidal cells. Ph.D. Thesis, University of California, Los Angeles.

Holt GR, Softky WR, Koch C, Douglas RJ (1996) Comparison of discharge variability in vitro and in vivo in cat visual cortex neurons. J. Neurophysiol. 75: 1806–1814.

Huguenard JR, Hamill OP, Prince DA (1988) Developmental changes in Na^+ conductances in rat neocortical neurons: Appearance of a slow inactivating component. J. Neurophysiol. 59: 778–795.

Johnston D, Magee JC, Colbert CM, Christie BR (1996) Active properties of neuronal dendrites. Annu. Rev. Neurosci. 19: 165–186.

Kisley MA, Gerstein GL (1999) The continuum of operating modes for a passive model neuron. Neural Comp. 11: 1139–1154.
Koch C, Laurent G (1999) Complexity and the nervous system. Science 284: 96–98.
König P, Engel AK, Roelfsema PR, Singer W (1995) How precise is neuronal synchronization? Neural Comp. 7: 469–485.
König P, Engel AK, Singer W (1996) Integrator or coincidence detector? The role of the cortical neuron revisited. Trends Neurosci. 19: 130–137.
Kretzberg J, Egelhaaf M, Warzecha A-K (2001) Membrane potential fluctuations determine the precision of spike timing and synchronous activity: A model study. J. Comp. Neurosci. 10: 79–97.
Krüger J, Becker JD (1991) Recognizing the visual stimulus from neuronal discharges. Trends Neurosci. 14: 282–286.
Lábos E (2000) Codes, operations, measurements and neural networks. Biosystems 58: 9–18.
Larkman AU (1991) Dendritic morphology of pyramidal neurons of the visual cortex of the rat. III. Spine distributions. J. Comp. Neurol. 306: 332–343.
Lytton WW (1996) Optimizing synaptic conductance calculation for network simulations. Neural Computation 8: 501–509.
MacGregor RJ (1991) Sequential configuration model for firing patterns in local neural networks. Biol. Cybern. 65: 339–349.
Magee JC (2000) Dendritic integration of excitatory synaptic input. Nature Rev. Neurosci. 1: 181–190.
Mainen ZF, Sejnowski TJ (1995) Reliability of spike timing in neocortical neurons. Science 268: 1503–1506.
Maršálek P, Koch C, Maunsell J (1997) On the relationship between synaptic input and spike output jitter in individual neurons. Proc. Natl. Acad. Sci. USA 94: 735–740.
McClurkin JW, Optican LM, Richmond BJ, Gawne TJ (1991) Concurrent processing and complexity of temporally encoded neuronal messages in visual perception. Science 253: 675–677.
Murthy VN, Fetz EE (1994) Effects of input synchrony on the firing rate of a three-compartment cortical neuron model. Neural Comp. 6: 1111–1126.
Noda H, Adey R (1970) Firing variability in cat association cortex during sleep and wakefulness. Brain Res. 18: 513–526.
Nowak LG, Sanchez-Vives MV, McCormick DA (1997a) Influence of low and high frequency inputs on spike timing in visual cortical neurons. Cereb. Cortex 7: 487–501.
Nowak LG, Sanchez-Vives MV, McCormick DA (1997b) Membrane potential trajectory preceding visually evoked action potentials in cat's visual cortex. Soc. Neurosci. Abstr. 23: 14.
Panzeri S, Petersen RS, Schultz SR, Lebedev M, Diamond ME (2001) The role of spike timing in the coding of stimulus location in rat somatosensory cortex. Neuron 29: 769–777.
Panzeri S, Schultz SR (2001) A unified approach to the study of temporal, correlational, and rate coding. Neural Comp. 13: 1311–1349.
Panzeri S, Schultz SR, Treves A, Rolls ET (1999) Correlations and the encoding of information in the nervous system. Proc. R. Soc. Lond. B Biol. Sci. 266: 1001–1012.
Paré D, Shink E, Gaudreau H, Destexhe A, Lang EJ (1998) Impact of spontaneous synaptic activity on the resting properties of cat neocortical neurons in vivo. J. Neurophysiol. 79: 1450–1460.
Prut Y, Vaadia E, Bergman H, Haalman I, Slovin H, Abeles M (1998) Spatiotemporal structure of cortical activity: Properties and behavioral relevance. J. Neurophysiol. 79: 2857–2874.
Reinagel P, Reid RC (2000) Temporal coding of visual information in the thalamus. J. Neurosci. 20: 5392–5400.
Riehle A, Grün S, Diesmann M, Aertsen A (1997) Spike synchronization and rate modulation differentially involved in motor cortical function. Science 278: 1950–1953.
Rudolph M, Destexhe A (2001a) Correlation detection and resonance in neural systems with distributed noise sources. Phys. Rev. Lett. 86: 3662–3665.
Rudolph M, Destexhe A (2001b) Do neocortical pyramidal neurons display stochastic resonance? J. Comp. Neurosci. 11: 19–42.
Schwindt PC, Crill WE (1997) Local and propagated dendritic action potentials evoked by glutamate iontophoresis on rat neocortical pyramidal neurons. J. Neurophysiol. 77: 2466–2483.
Segundo JP (2000) Some thoughts about neural coding and spike trains. Biosystems 58: 3–7.
Segundo JP, Perkel DH, Moore GP (1966) Spike probability in neurones: Influence of temporal structure in the train of synaptic events. Kybernetik 3: 67–82.
Shadlen MN, Newsome WT (1994) Noise, neural codes and cortical organization. Curr. Opin. Neurobiol. 4: 569–579.
Shadlen MN, Newsome WT (1995) Is there a signal in the noise? Curr. Opin. Neurobiol. 5: 248–250.
Shadlen MN, Newsome WT (1998) The variable discharge of cortical neurons: Implications for connectivity, computation, and information coding. J. Neurosci. 18: 3870–3896.
Shinomoto S, Sakai Y, Funahashi S (1999) The Ornstein-Uhlenbeck process does not reproduce spiking statistics of neurons in prefrontal cortex. Neural Comput. 11: 935–951.
Smith DR, Smith GK (1965) A statistical analysis of the continuous activity of single cortical neurons in the cat unanesthetized isolated forebrain. Biophys. J. 5: 47–74.
Softky WR (1994) Sub-millisecond coincidence detection in active dendritic trees. Neuroscience 58: 13–41.
Softky WR (1995) Simple codes versus efficient codes. Curr. Opin. Neurobiol. 5: 239–247.
Softky WR, Koch C (1993) The highly irregular firing of cortical cells is inconsistent with temporal integration of random EPSPs. J. Neurosci. 13: 334–350.
Stein RB (1967) Some models of neuronal variability. Biophys. J. 7: 37–68.
Stevens CF, Zador AM (1998) Input synchrony and the irregular firing of cortical neurons. Nature Neurosci. 1: 210–217.
Stuart G, Spruston N, Sakmann B, Häusser M (1997) Action potential initiation and backpropagation in neurons of the mammalian CNS. Trends Neurosci. 20: 125–131.
Theunissen F, Miller JP (1995) Temporal encoding in nervous systems: A rigorous definition. J. Comput. Neurosci. 2: 149–162.
Tovée MJ, Rolls ET, Treves A, Bellis RP (1993) Information encoding and the responses of single neurons in the primate temporal visual cortex. J. Neurophysiol. 70: 640–654.
Traub RD, Miles R (1991) Neuronal Networks of the Hippocampus. Cambridge University Press.
Troyer TW, Miller KD (1997) Physiological gain leads to high ISI variability in a simple model of a cortical regular spiking cell. Neural. Comp. 9: 971–983.
Tsodyks MV, Sejnowski T (1995) Rapid state switching in balanced cortical network models. Network 6: 111–124.
Usher M, Stemmler M, Koch C, Olami Z (1994) Network amplification of local fluctuations causes high spike rate variability, fractal

firing patterns and oscillatory local field potentials. Neural. Comp. 6: 795–836.

Vaadia E, Haalman I, Abeles M, Bergman H, Prut Y, Slovin H, Aertsen A (1995) Dynamics of neuronal interactions in monkey cortex in relation to behavioural events. Nature 373: 515–518.

van Vreeswijk C, Sompolinsky H (1996) Chaos in neuronal networks with balanced excitatory and inhibitory activity. Science 274: 1724–1726.

White EL (1989) Cortical Circuits. Birkhauser. Boston.

Zohary E, Shadlen MN, Newsome WT (1994) Correlated neuronal discharge rate and its implications for psychophysical performance. Nature 370: 140–143.